BMC Genomics

RESEARCH

Open Access

Whole-genome resequencing reveals melanin deposition candidate genes of Luning chicken

Chuwen Chen[1,2,3], Jie Li[1,2,3], Zhiyi Li[1,2,3], Yi Nong[1,2,3], Jiayan Wang[1,2,3], Zi Wang[1,2,3] and Zhixiong Li[1,2,3*]

Abstract

Background Melanin in the black-bone chicken's body is considered the material basis for its medicinal effects and is an economically important trait. Therefore, improving the melanin content is a crucial focus in the breeding process of black-bone chickens. Luning chickens are black-bone chickens, with black beaks, skin, and meat. To investigate the genetic diversity and molecular mechanisms of melanin deposition in Luning chickens, we conducted whole-genome resequencing to analyze their breeding history and identify candidate genes influencing their black phenotype, along with transcriptome sequencing of dorsal skin tissues of male Luning chickens.

Results Population structure analysis revealed that Luning chickens tend to cluster independently and are closely related to Tibetan chickens. Runs of homozygosity analysis suggested potential inbreeding in the Luning chicken and Tibetan chicken population. By combining genetic differentiation index (*Fst*) and nucleotide diversity ($\theta\pi$) ratios, we pinpointed selected regions associated with melanin deposition. Gene annotation identified 540 genes with the highest *Fst* value in *LOC101750371* and *LOC121108313*, located on the 68.24–68.58 Mb interval of chromosome Z. Combining genomic and transcriptomic data, we identified *ATP5E*, *EDN3*, and *LOC101750371* as candidate genes influencing skin color traits in black-bone chickens.

Conclusions This study characterized the evolutionary history of Luning chickens and preliminarily excavated candidate genes influencing the genetic mechanism of pigmentation in black-bone chickens, providing valuable insights for the study of animal melanin deposition.

Keywords Luning chicken, Genetic diversity, Integration of whole-genome and transcriptome, Selective sweep, Melanin

Background

Domestication is a mutually beneficial co-evolutionary process that enhances the survival adaptations of both domesticators and the domesticated. It marks a crucial shift in human lifestyle from hunting to pastoralism [1]. This process leads to genetic differentiation and diversification, increasing the breeds' productivity and adaptability to the environment, and promoting phenotypic diversity in terms of morphology and color [2, 3].

The chicken (*Gallus Gallus domesticus*) has been an early domesticated agricultural economic animal, providing a stable source of animal protein for humans. They

*Correspondence:
Zhixiong Li
lizhixiong@swun.edu.cn
[1]Key Laboratory of Qinghai-Tibetan Plateau Animal Genetic Resource Reservation and Utilization (Southwest Minzu University), Ministry of Education, Chengdu, China
[2]Key Laboratory of Animal Science of National Ethnic Affairs Commission of China, Southwest Minzu University, Chengdu, China
[3]College of Animal & Veterinary Sciences, Southwest Minzu University, Chengdu, China

exhibit significant phenotypic diversity, with different breeds distinguished by phenotypic characteristics such as body size, plumage or skin color, and crown type [4]. The black-bone trait is an important indicator in the chicken domestication process. According to the *Compendium of Materia Medica* and the *Medicinal Fauna of China*, black-bone chickens process various medicinal properties and has been widely used in pharmaceuticals [5], nutritional supplements [6], and immune support [7]. The melanin content determines the shade of color and affects the economic benefits of black-bone chicken in China. Therefore, breeders aim to achieve melanin coloration during the breeding of black-bone chickens.

The Luning chicken originates from Mianning County, Sichuan Province, China. It has well-developed pectoral/leg muscles and high egg-laying performance, characterized by black beaks, skin, and meat. Situated in the mountainous terrain of Liangshan Yi Autonomous Prefecture in Sichuan Province, Mianning County has promoted the Luning chicken as a valuable economic resource to boost local livestock production. Despite its popularity among consumers, the Luning chicken faced extinction in the past due to various factors, and its breeding history remains poorly documented. Therefore, exploring the Luning chicken at the genomic level is crucial to understanding the genetic mechanisms of melanin deposition. Whole-genome resequencing (WGRS) stands out for its precision, reproducibility, and accuracy, making it a preferred method for identifying candidate genes associated with essential traits in livestock and poultry species like chickens [8, 9], pigs [10, 11], cattle [12], sheep [13, 14], ducks [15] and geese [16].

In this study, the whole genomes of 5 Luning chickens were sequenced. Based on the genomic data of Luning chickens, we employed WGRS to uncover the actual composition of the Luning chicken population. This revealed insights into population structure, evolutionary history, and genomic diversity for characterization, as well as the identification of genes that have undergone positive selection in the evolutionary journey of the Luning chicken based on genomic diversity. Furthermore, we delved into the genetic foundation of melanin deposition through an integrated analysis of genomic and transcriptome sequencing (RNA-seq) data. This study contributes to the preservation of the indigenous Luning chicken breeds and the advancement of germplasm resources, offering fundamental research data for the selection and enhancement of Luning chicken breed.

Results

Genetic variation in Luning chicken

We performed WGRS of 5 Luning chickens. Utilizing the pre-processing tool fastp to filter low-quality sequences from the raw data, we obtained a total of 185 Gb of high-quality genomic data, with each chicken contributing over 30 Gb per chicken (Supplementary Table S1). The Q30 scores exceeded 84%, and the average GC content was 41.46%. When aligning the obtained sequences to the chicken reference genome (GRCg7b), the mapping rate was over 99.78%, with an average sequencing depth of 34× per individual (Supplementary Table S2). Following accurate quality filtering of the identified SNPs and InDels, we discovered 35,436,078 SNPs and 4,734,764 InDels (Supplementary Table S3 & Supplementary Table S4). Figure 1b illustrates the Circos map integrating the SNPs and InDels loci of LNC1, while the Circos map of the remaining 4 Luning chicken individuals are displayed in Supplementary Fig. S1. To visualize the distribution of SNPs more effectively, we categorized them into 11 groups based on their context (Fig. 1c). The majority of these SNPs were located in intergenic (36.71%) and intronic (52.12%) regions, with only 1.63% in exonic regions. Additionally, 4.19% were found in 5´and 3´UTRs, and 5.15% in upstream and downstream regions. A smaller proportion of SNPs were within ncRNA genes (0.21%) and splicing regions (0.01%).

Phylogeny and population genetic structure as well as migration events

We analyzed genome-wide and evolutionary relationships between Luning chickens and other breeds based on 40 individual genomic-wide SNPs (Fig. 1a, Supplementary Table S5). The heat map revealed two primary genetic clusters, with SC forming a separate category and the remaining seven varieties clustered together. Cluster analysis revealed that the JBC samples exhibited more variation among themselves, while the other 7 breeds showed a smaller degree of variation and were more closely related evolutionarily (Fig. 1d). We employed the NJ algorithm to calculate genetic distances between populations based on genome-wide polymorphic SNPs in 8 breeds and construct a phylogenetic tree (Fig. 2a). LNC clustered within the same branch as TBC, RJF, MBC, and XBC, showing the nearest genetic distance to TBC. Interesting, JBC is divided into three branches. The JBC population from PCA analysis showed individuals mixed with MBC and RJF, respectively, with RJF further divided into two parts. Additionally, the other 6 breeds formed distinct clusters with a high level of genetic differentiation (Fig. 2b). The four principal components PC1, PC2, PC3, and PC4 each accounted for 7.41%, 5.22%, 4.75%, and 4.05% of the total variability.

To estimate the ancestral proportions of the eight chicken breeds, we performed Admixture analysis on 40 sampled chickens, with K representing the number of assumed ancestral populations (Fig. 2c). The optimal choice for the current 40 samples was determined to be is K=2, based on the lowest Cross Validation error

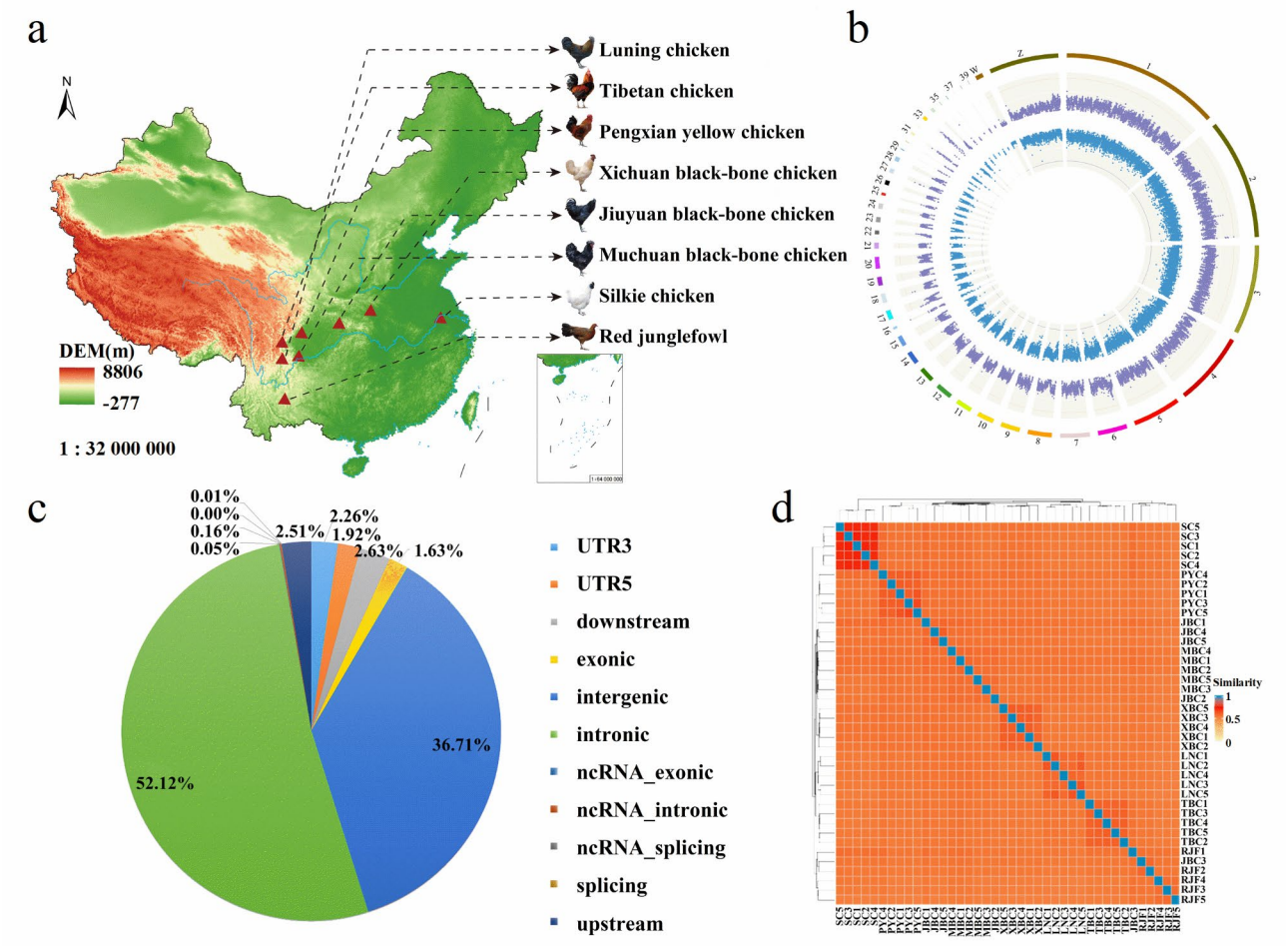

Fig. 1 Experiment design and variant statistic. (**a**) Geographical origin of the 8 chicken breeds used in this study. The map is made based on the standard map with the review number GS (2016) 1569 downloaded from the standard map service station of the Ministry of Natural Resources, and the base map is unmodified. (**b**) Circos map of genomic variation. Chromosomes are represented in different colors in the outermost circle, purple loci indicate the distribution of genomic SNP densities, and blue loci indicate the distribution of genomic InDel densities. (**c**) SNP distribution pie chart. Different colors represent SNPs within various functional regions, this pie chart represents the total SNPs. (**d**) SNPs distribution map of 40 samples. Heat map of the differential distribution of SNPs based on genomic data from 40 chickens of 8 breeds, colors represent pairwise genetic distance

(Supplementary Fig. S2). At K=2, LNC exhibited a similar pedigree composition to TBC, while SC tended to cluster independently, and the other 5 populations genetically fell into one cluster. Furthermore, at K=2, different genetic clusters were clearly formed within the JBC population, consistent with the NJ tree and PCA results. Based on the above analysis, the correlation between the JBC samples was low, potentially affecting the accuracy of the results, leading to their exclusion from subsequent analyses. ROH refers to a class of genomes exhibiting continuous uninterrupted pure heterozygosity, characterized by the absence of heterozygotes in one chromosomal region [17]. By comparison of ROH, we revealed higher ROH values and lower heterozygosity among LNC and TBC (Fig. 2d, Supplementary Fig. S3). This result is consistent with the phenomenon that TBC and LNC as local breeds tend to be inbred in relatively closed areas. We divided the populations into black-bone (LNC, XBC, MBC, and SC) and non-black-bone (TBC, PYC, and RJF) groups for the LD analysis. As shown in Fig. 2e, there was no significant difference in the decay rate between the black-bone and the non-black-bone.

Analysis of demographic history

The historical effective population size (Ne) was estimated based on SNPs in the whole genome of LNC and other Chinese chicken breeds using MSMC2, a successor to the MSMC. The results indicated highly similar patterns of population trajectories among the seven breeds (Fig. 3). The population sizes of the seven chicken breeds appeared to increase slowly at 10 Mya, reaching a peak at about 1 Mya, showing a slow decline up to the Last Interglacial (LIG; 130–115 kya), followed by a sharp decline. The sudden decrease in population size may be linked to

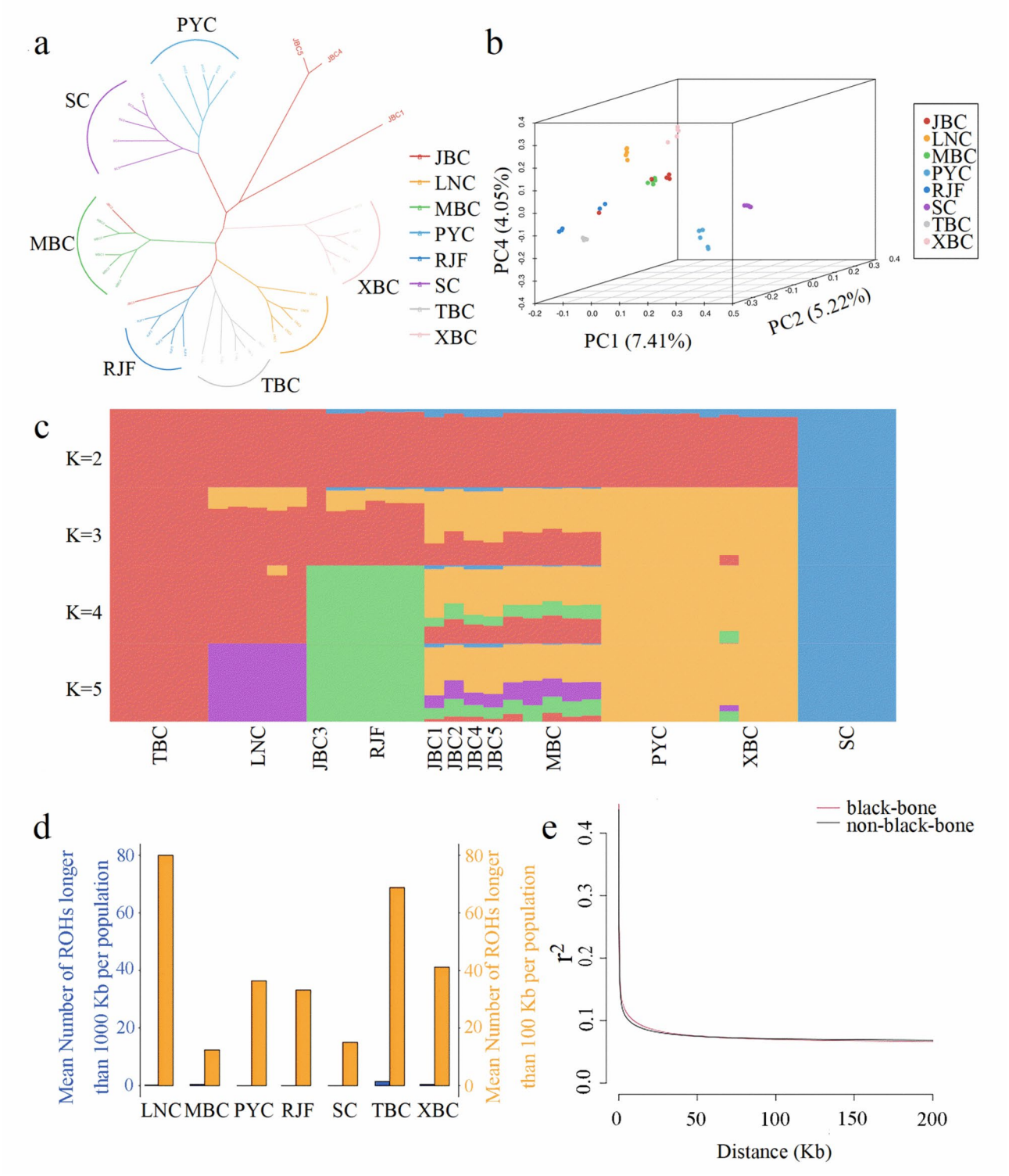

Fig. 2 Analysis of population variation and structure of the LNC and their relatives. (**a**) NJ tree was constructed using polymorphisms detected in the 40 individual chickens. (**b**) Three-way principal component plots of the 40 individuals. (**c**) Population structure of samples from 40 individuals examined via the program ADMIXTURE. K is the number of presumed genetic clusters, and K = 2 is the best. (**d**) The frequency of ROH in each breed. (**e**) Decay of black-bone and non-black-bone chickens measured by r^2. The horizontal coordinate is the physical distance (Kb) and the vertical coordinate is the LD r^2, which takes a value in the range of 0 to 1, with higher values indicating a higher degree of linkage disequilibrium between loci

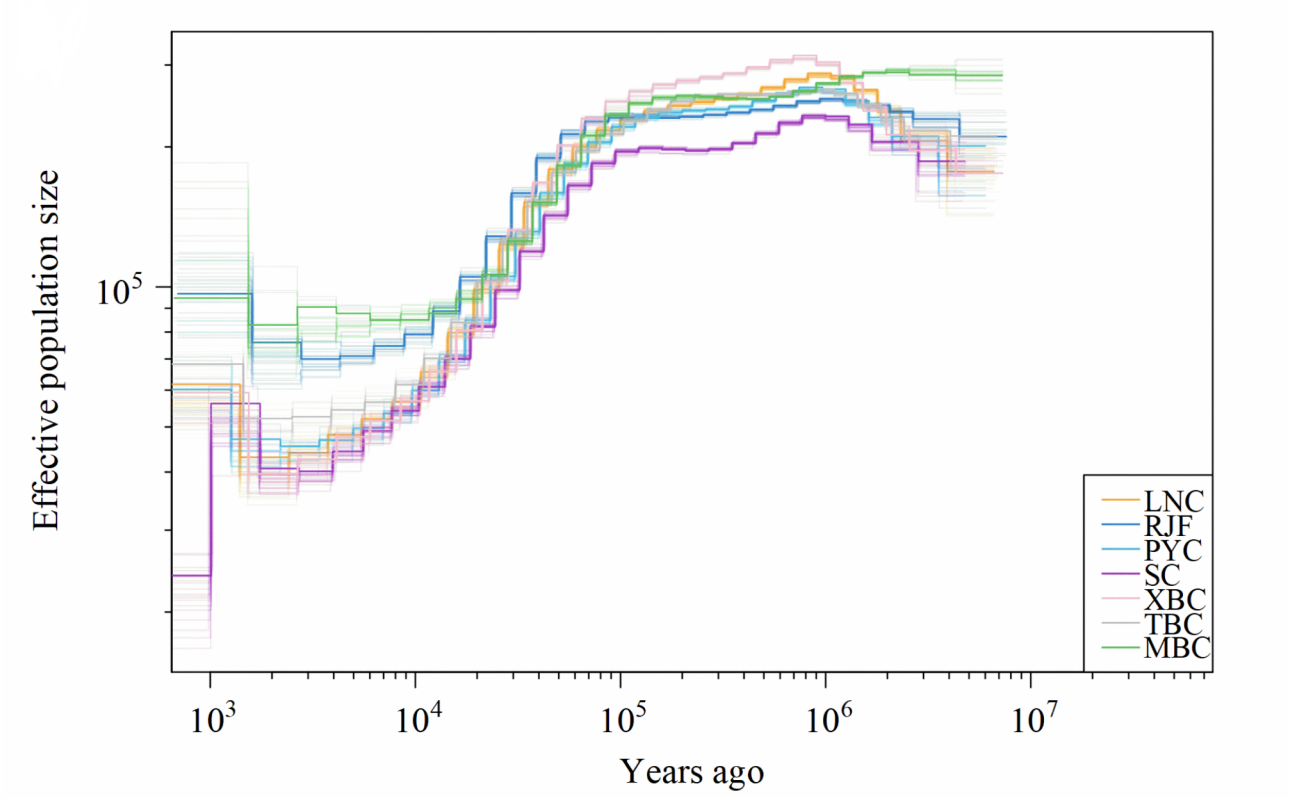

Fig. 3 Demographic history of the chicken population. Demographic history of the 35 individuals with MSMC2 analysis based on SNP distribution. Generation time (g) = 1 year and neutral mutation rate per generation (μ) = 1.91×10^{-9}

extreme temperature and aridity disaster that occurred during the Last Glacial Maximum (LGM; 20-26.5 kya) [18, 19].

Genome-wide selective sweep signals and functional analysis

To enhance the detection of genome-wide selection signatures linked to melanin deposition, we divided populations into black-bone and non-black-bone groups based on previous classification. *Fst* value and $\theta\pi$ Ratios were calculated for SNP variant loci and displayed as Manhattan plots (Fig. 4b and c). Moreover, the top 5% of the *Fst* value (≥0.066) and the top 5% of the $\theta\pi$ ratios (< -0.071 or >0.366) were utilized as criteria for classifying selective sweeps (Fig. 4a). Within these sweeps, gene annotation identified 540 genes with the highest *Fst* value in *LOC101750371* and *LOC121108313* located on the 68.24–68.58 Mb interval of chromosome Z (chrZ) (Supplementary Table S6). Besides, numerous genes associated with pigmentation were detected in the top 200 regions, including ATP synthase, H+transporting, mitochondrial F1 complex, epsilon subunit (*ATP5E*), Endothelin3 (*EDN3*), engulfment and cell motility 2 (*ELMO2*), GNAS complex locus (*GNAS*), tubulin beta 1 class VI (*TUBB1*), methylthioadenosine phosphorylase (*MTAP*), cyclin dependent kinase inhibitor 2 A (*CDKN2A*), cyclin dependent kinase inhibitor 2B (*CDKN2B*), tripartite motif containing 36 (*TRIM36*), neuregulin 1 (*NRG1*), cathepsin V (*CTSV*), FER tyrosine kinase (*FER*). Furthermore, the $\theta\pi$ ratio in the black-bone group ($\theta\pi$=0.00383) was lower than the non-black-bone group ($\theta\pi$=0.00395), suggesting that a sweep has been positively selected in the black-bone group (Supplementary Table S7). Genes undergoing selection between black-bone and non-black-bone chickens were subjected to GO functional enrichment analysis. The top 30 of the analysis revealed 10 GO terms enriched in biological processes, 10 terms in cellular components, and 10 terms in molecular functions (Supplementary Fig. S4). In addition, 28 GO terms (P<0.05) associated with melanin deposition were filtered out (Table 1). A total of 24 genes were enriched for these terms, including G protein subunit alpha q (*GNAQ*), KIT ligand (*KITLG*), melanin-concentrating hormone receptor 1 (*MCHR1*), and tyrosinase (*TYR*) known to play a crucial role in the regulation of melanin deposition.

RNA-seq data

To compare skin color differences, we individually determined the L-values of the dorsal skin of four male Luning chickens. The L-values of black skin (BS) averaged around 46, while the L-value of white skin (WS) was 64,

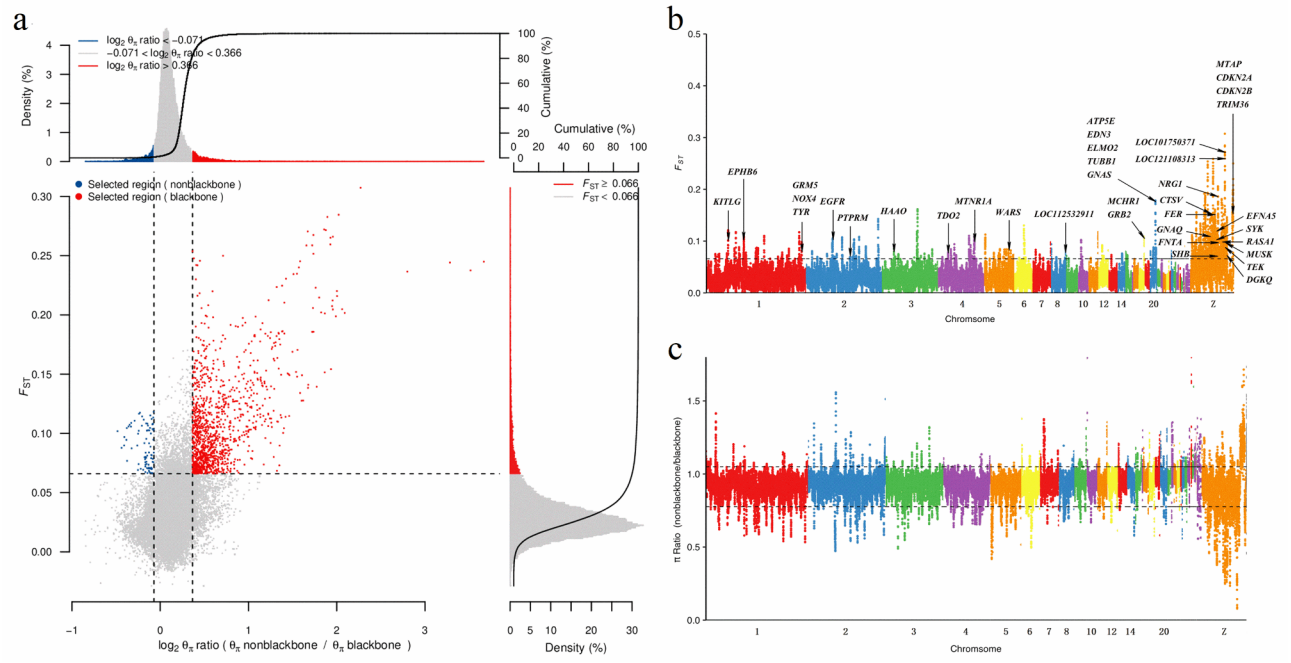

Fig. 4 Identification of genomic regions in Luning chickens with positive selection scans. (**a**) The horizontal coordinates represent the $\log_2\theta\pi$ ratio ($\theta\pi$ non-black-bone / $\theta\pi$ black-bone) and the vertical coordinates represent the *Fst* values, which correspond to the top and right density distribution. Regions selected for the non-black-bone are shown using blue points, while black-bone are shown in red. (**b**) Population differentiation distribution map of *Fst*. The dashed line indicates the *Fst* top5% threshold, the horizontal coordinate indicates the chromosome and the vertical coordinate indicates the *Fst* value. (**c**) Analysis of $\theta\pi$ between non-black-bone group and black-bone group of chicken

showing a highly significant difference (Supplementary Table S8). To understand the genetic influence on melanin deposition in Luning chickens, we performed a differential expression analysis of mRNAs, lncRNAs, and pre-miRNAs in the dorsal skin tissues of WS and BS chickens. The results revealed significant differences in expression levels with 2045 mRNAs (1140 upregulated and 905 downregulated), 2762 lncRNAs (1995 upregulated and 767 downregulated), and 110 pre-miRNAs (22 upregulated and 88 downregulated) in WS and BS tissues (Fig. 5a, b and c). Moreover, 1506 target genes were identified from 2762 DE lncRNAs, 66 of which were involved in both cis-acting and trans-acting. Furthermore, 110 DE pre-miRNAs targeted a total of 7767 target genes. GO analysis of the DE mRNAs and DE lncRNAs target genes revealed 11 and 12 enriched GO terms related to pigmentation, respectively, while no pigmentation related terms were found in the enrichment results for DE pre-miRNAs target genes (Tables 2 and 3).

Candidate genes for melanin deposition

Based on the above results, we performed a combined analysis of WGRS and RNA-seq to identified candidate genes influencing melanin deposition in chickens. In the WGRS analysis, we compared black-bone chickens and non-black-bone chickens to detect candidate genes associated with melanin deposition. A total of 412 genes out of 540 genes in the selected region were strongly selected ($P_{adj} < 0.05$). These selected genes overlapped 50 genes with DE mRNAs, 37 DE lncRNAs target genes, and 199 DE pre-miRNAs target genes in the RNA-seq, respectively. Notably, 29 genes were found to be co-occurring in these four datasets, includes candidate genes from the previous WGRS analysis: *ATP5E*, *EDN3*, and *LOC101750371* (Fig. 5d). Particularly, *LOC101750371* was most strongly selected in the selective sweep. Consequently, *ATP5E*, *EDN3*, and *LOC101750371* were selected as potential candidate genes influencing melanin deposition in chickens.

Validation of RNA-seq results by qRT-PCR

To validate the expression levels of DE mRNAs, DE lncRNAs, and DE pre-miRNAs observed in RNA-seq, we performed qRT-PCR on 5 randomly selected transcripts from each group. The results demonstrated that the expression trends from both qRT-PCR and RNA-seq were consistent, validating the reliability and accuracy of the RNA-seq results (Fig. 6).

Cloning and analysis of the Luning chicken *LOC101750371* gene

Successful cloning of the CDS sequence of Luning chicken *LOC101750371* gene (2055 bp) revealed that the gene is predicted to encode 684 amino acids

Table 1 GO terms associated with melanin deposition in GO enrichment analysis of WGRS ($P < 0.05$)

GO id	Term	Category	*P* value	Gene
GO:0045634	regulation of melanocyte differentiation	BP	0	*GNAQ*
GO:0004833	tryptophan 2,3-dioxygenase activity	MF	0	*TDO2*
GO:1904408	melatonin binding	MF	0.00106	*MTNR1A*
GO:0030273	melanin-concentrating hormone receptor activity	MF	0.00106	*MCHR1*
GO:0019442	tryptophan catabolic process to acetyl-CoA	BP	0.00106	*TDO2*
GO:0004830	tryptophan-tRNA ligase activity	MF	0.00106	*WARS*
GO:0006436	tryptophanyl-tRNA aminoacylation	BP	0.00106	*WARS*
GO:0030296	protein tyrosine kinase activator activity	MF	0.00106	*GRM5*
GO:1990782	protein tyrosine kinase binding	MF	0.00114	*NOX4*; *GRM5*; *RASA1*
GO:0018108	peptidyl-tyrosine phosphorylation	BP	0.00189	*EGFR*; *SYK*; *FER*; *TEK*
GO:0006569	tryptophan catabolic process	BP	0.00310	*HAAO*
GO:0019441	tryptophan catabolic process to kynurenine	BP	0.00310	*TDO2*
GO:1900086	positive regulation of peptidyl-tyrosine autophosphorylation	BP	0.00310	*LOC112532911*
GO:0034354	'de novo' NAD biosynthetic process from tryptophan	BP	0.00607	*HAAO*
GO:0030297	transmembrane receptor protein tyrosine kinase activator activity	MF	0.00607	*DGKQ*
GO:0004714	transmembrane receptor protein tyrosine kinase activity	MF	0.00740	*EPHB6*; *EGFR*; *MUSK*; *TEK*
GO:0050731	positive regulation of peptidyl-tyrosine phosphorylation	BP	0.00920	*KITLG*; *EFNA5*; *RASA1*; *DGKQ*
GO:0061098	positive regulation of protein tyrosine kinase activity	BP	0.00954	*NOX4*; *GRM5*
GO:0045636	positive regulation of melanocyte differentiation	BP	0.00990	*KITLG*
GO:0008502	melatonin receptor activity	MF	0.00990	*MTNR1A*
GO:0048066	developmental pigmentation	BP	0.00990	*GNAQ*
GO:0042438	melanin biosynthetic process	BP	0.01453	*TYR*
GO:0043473	pigmentation	BP	0.01991	*TYR*
GO:0033162	melanosome membrane	CC	0.03270	*TYR*
GO:0030971	receptor tyrosine kinase binding	MF	0.03713	*ELMO2*; *FNTA*; *RASA1*
GO:0050730	regulation of peptidyl-tyrosine phosphorylation	BP	0.04000	*EGFR*
GO:0005001	transmembrane receptor protein tyrosine phosphatase activity	MF	0.04000	*PTPRM*
GO:0001784	phosphotyrosine residue binding	MF	0.04634	*GRB2*; *SHB*

(Supplementary Fig. S5). Bioinformatics analysis of the LOC101750371 protein was conducted and shown in Supplementary Fig. S6.

The mRNA expression of *LOC101750371* was detected in 8 tissues (heart, liver, spleen, lung, kidney, pectoral muscle, leg muscle, and dorsal skin) of black-skin Luning chickens using qRT-PCR (Fig. 7). The results indicated that *LOC101750371* was expressed in all tissues, with significantly higher expression in the dorsal skin compared to the other 7 tissues, followed by the pectoral muscle and leg muscle. To further explore the molecular characteristics of *LOC101750371* gene, qRT-PCR was utilized to compare its expression in all 8 tissues of white-skin Luning chickens and black-skin Luning chickens (Fig. 8). The findings revealed that the expression difference in the pectoral muscle, leg muscle, dorsal skin and kidney tissues between white-skin and black-skin Luning chickens was significant.

Discussion

The Luning chicken, a unique breed identified in the 1980s and listed in the *National Breed List of Livestock and Poultry Genetic Resources*, has evolved into an excellent local breed for meat and eggs through artificial and natural selection. However, there has been little research on their phenotypic traits and genetic improvement. In this research, we sequenced the genomes of 5 Luning chickens to explore their population structure, analyze genetic differences, and examine their population history in comparison to other local chicken breeds.

Genetic evolutionary analysis using SNP sites of eight breeds revealed that geographically proximate chickens tended to cluster together, consistent with previous studies [20, 21]. Population structure analysis through PCA, NJ tree, and Admixture analysis indicated diverse affinities among JBC breeds, possibly due to the different domestication venues or multiple genetic origins [22, 23]. PCA and NJ tree analyses showed consistent results, with all varieties clustering independently except for JBC. Admixture analysis was consistent with the results of cluster analysis, with SC being the first to be distinguished from the other varieties. The ROH results indicated that LNC had the highest long ROH values, possibly due to active conservation efforts in recent years, which may explain the low genetic diversity of LNC [17, 24]. LD decay analysis indicated no significant difference in attenuation rates among black-bone chickens and non-black-bone chickens, suggesting similar selection

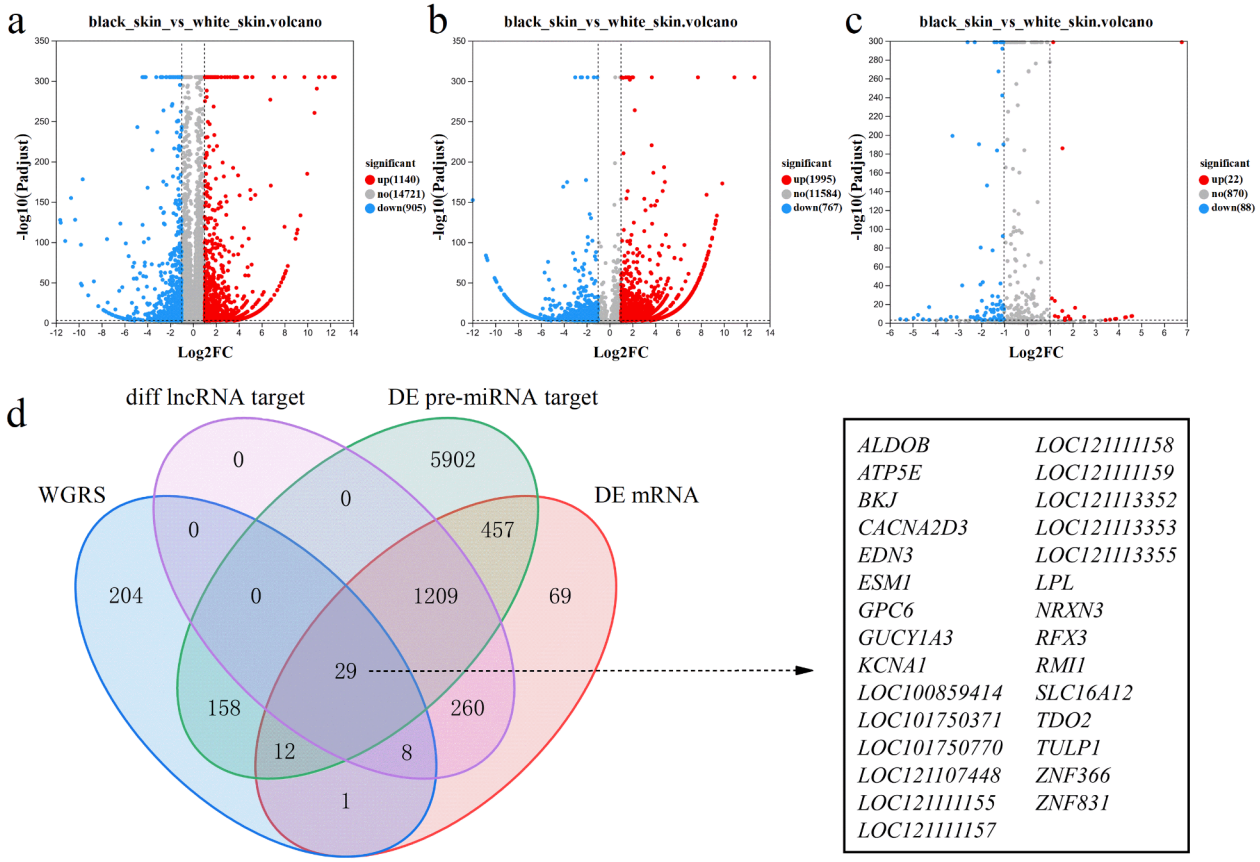

Fig. 5 Differentially expressed RNAs of black and white skin Luning chickens. Volcano plot of differentially expressed mRNAs (**a**), lncRNAs (**b**), and pre-miRNAs (**c**) in WS and BS. Red points represent upregulation, gray points represent insignificant differences, and blue points represent downregulation in volcano plots. Differentially expressed RNAs with P_{adj} values too small to be presented in the volcano plots were plotted uniformly on -Log_{10} (P_{adj}) = 300. (**d**) Integration analysis of WGRS and RNA-seq. Venn diagram of strongly selected genes in WGRS and differentially expressed genes (DE mRNAs, DE lncRNAs target genes, and DE pre-miRNAs target genes) in RNA-seq

Table 2 GO terms associated with melanin deposition in GO enrichment analysis of DE mRNAs ($P < 0.05$)

GO id	Term	Category	*P* value	Gene
GO:0042438	melanin biosynthetic process	BP	0.00432	*DCT*; *ASIP*; *TYR*; *TYRP1*
GO:0006582	melanin metabolic process	BP	0.00432	*DCT*; *ASIP*; *TYR*; *TYRP1*
GO:0032438	melanosome organization	BP	0.00787	*RAB38*; *ASIP*; *PMEL*; *TYRP1*
GO:0033162	melanosome membrane	CC	0.00787	*RAB38*; *DCT*; *TYR*; *TYRP1*
GO:0048753	pigment granule organization	BP	0.00787	*RAB38*; *ASIP*; *PMEL*; *TYRP1*
GO:0090741	pigment granule membrane	CC	0.00787	*RAB38*; *DCT*; *TYR*; *TYRP1*
GO:0042470	melanosome	CC	0.01800	*GCHFR*; *DCT*; *PMEL*; *TYR*; *HSP90AA1*; *MLANA*; *TYRP1*
GO:0048770	pigment granule	CC	0.01800	*GCHFR*; *DCT*; *PMEL*; *TYR*; *HSP90AA1*; *MLANA*; *TYRP1*
GO:0048023	positive regulation of melanin biosynthetic process	BP	0.03554	*ASIP*; *TYRP1*
GO:0008502	melatonin receptor activity	MF	0.03554	*RORB*; *MTNR1B*
GO:0043473	pigmentation	BP	0.04499	*DCT*; *EN1*; *SLC45A2*; *TYR*; *TYRP1*

intensities. MSMC2 analysis revealed that the effective population of seven chicken breeds is influenced by environmental changes, and the correlation with environmental conditions indicated that the effective population size is related to the breeds´ adaptation to the environment [25].

In recent years, WGRS technology has been extensively used in biological studies to detect variations in genomes, aiming to identify potential functional genes associated with traits and reveal the genetic mechanisms of natural and artificial selection in livestock and poultry. Currently, numerous candidate genes related to traits have

Table 3 GO terms associated with melanin deposition in GO enrichment analysis of DE lncRNAs ($P < 0.05$)

GO id	Term	Category	*P* value	Gene
GO:0042438	melanin biosynthetic process	BP	0.00170	*DCT*; *ASIP*; *TYR*; *TYRP1*
GO:0006582	melanin metabolic process	BP	0.00170	*DCT*; *ASIP*; *TYR*; *TYRP1*
GO:0032438	melanosome organization	BP	0.00317	*RAB38*; *ASIP*; *PMEL*; *TYRP1*
GO:0033162	melanosome membrane	CC	0.00317	*RAB38*; *DCT*; *TYR*; *TYRP1*
GO:0048753	pigment granule organization	BP	0.00317	*RAB38*; *ASIP*; *PMEL*; *TYRP1*
GO:0090741	pigment granule membrane	CC	0.00317	*RAB38*; *DCT*; *TYR*; *TYRP1*
GO:0042470	melanosome	CC	0.00478	*GCHFR*; *DCT*; *PMEL*; *TYR*; *HSP90AA1*; *MLANA*; *TYRP1*
GO:0048770	pigment granule	CC	0.00478	*GCHFR*; *DCT*; *PMEL*; *TYR*; *HSP90AA1*; *MLANA*; *TYRP1*
GO:0043473	pigmentation	BP	0.01722	*DCT*; *EN1*; *SLC45A2*; *TYR*; *TYRP1*
GO:0048023	positive regulation of melanin biosynthetic process	BP	0.02201	*ASIP*; *TYRP1*
GO:0030318	melanocyte differentiation	BP	0.03850	*KIT*; *TYRP1*; *SOX10*
GO:0050931	pigment cell differentiation	BP	0.03850	*KIT*; *TYRP1*; *SOX10*

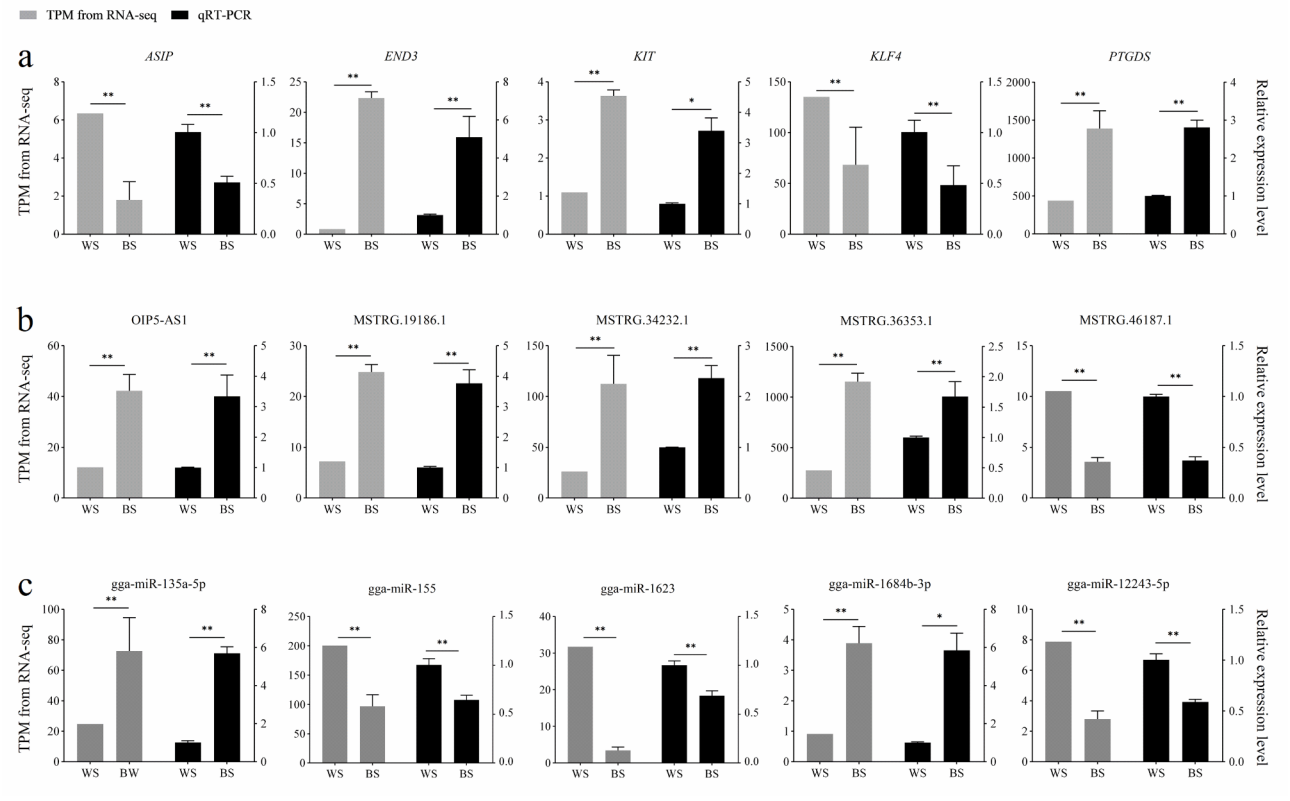

Fig. 6 Verification of the RNA-seq via qRT-PCR. The expression levels of five DE mRNAs (**a**), five DE lncRNAs (**b**), and five DE pre-miRNAs (**c**) were validated with qRT-PCR in the dorsal skin of Luning chickens. WS represents the white skin, and BS represents the black skin. *$P < 0.05$, **$P < 0.01$

been identified using genome-wide variation information, such as duck beak color [26], sheep litter size [27], and goose wing length [28], among others. Chicken skin color is an economically important trait, with consumers favoring black-bone chickens due to their suggested nutritional and medicinal value [29]. There is not insufficient scientific evidence to suggest that sex directly contributes to differences in melanin deposition. Our review of the literature revealed two reports with contrasting results: one study reported higher expression levels of *DCT*, *TYRP1*, and *TYR* (enzymes regulating enzymes involved in melanin synthesis) genes in male chickens compared to female chickens [30], and another study reported lower expression levels of *TYRP1* gene in male black-bone chickens than in females [31]. Thus at present, more investigation is needed to explore the role of sex in determining skin color. In order to avoid the error caused by sex, we selected male Luning chicken samples for both WGRS and RNA-seq. Several studies have shown that chromosome 20 (chr20) and chrZ play vital roles in skin color pigmentation. Li et al. [32] conducted a genome-wide association study, refining the dermal

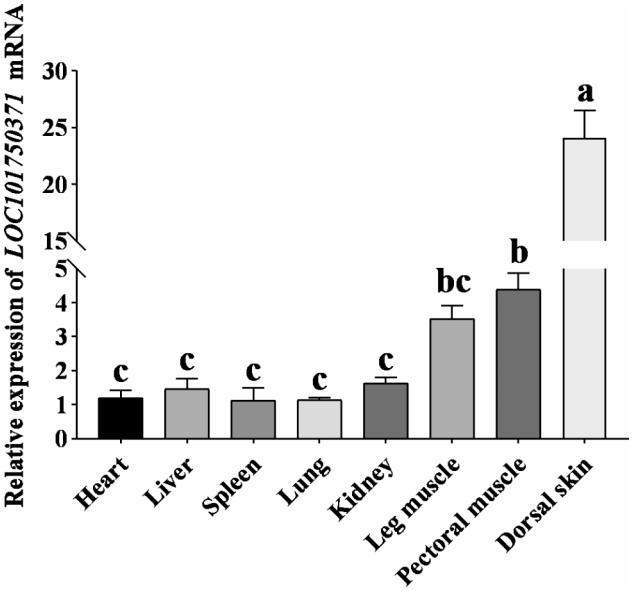

Fig. 7 Relative expression of *LOC101750371* gene in different tissues of black skin Luning chicken. Different lowercase letters represent significant difference ($P < 0.05$)

melanin inhibitor gene (Id) location and identifying 3 significant SNPs located at 78.5–79.2 Mb on chrZ associated with dermal calf pigmentation in Tibetan chickens. Hou et al. [33] employed a combination of genome-wide association study and *Fst* scan to identify 68 SNPs on chr20, mapping to 10 genes associated with dermal hyperpigmentation. Moreover, another study SNPs significantly linked to chicken skin color pigmentation in a ~ 2.94 Mb region on chrZ and ~ 3.58 Mb region on chr20 [34]. A recent study exploring the mechanisms controlling eggshell and shank pigmentation in Italian local chickens by genome-wide association analysis [35]: revealed that concerning shank color, a SNP with an exceptionally low *P* value was identified in the 31 Mb region of chrZ, and another SNP from the same genomic region was also located in *NFIB* (near the *TYRP1* gene), a region known to be associated with dark skin color and shank [30, 36]. This study utilized the intersection of the top 5% *Fst* and $\theta\pi$ ratio to determine the genome region under selection and analyzed the screened candidate genes for enrichment. The results aligned with previous findings,

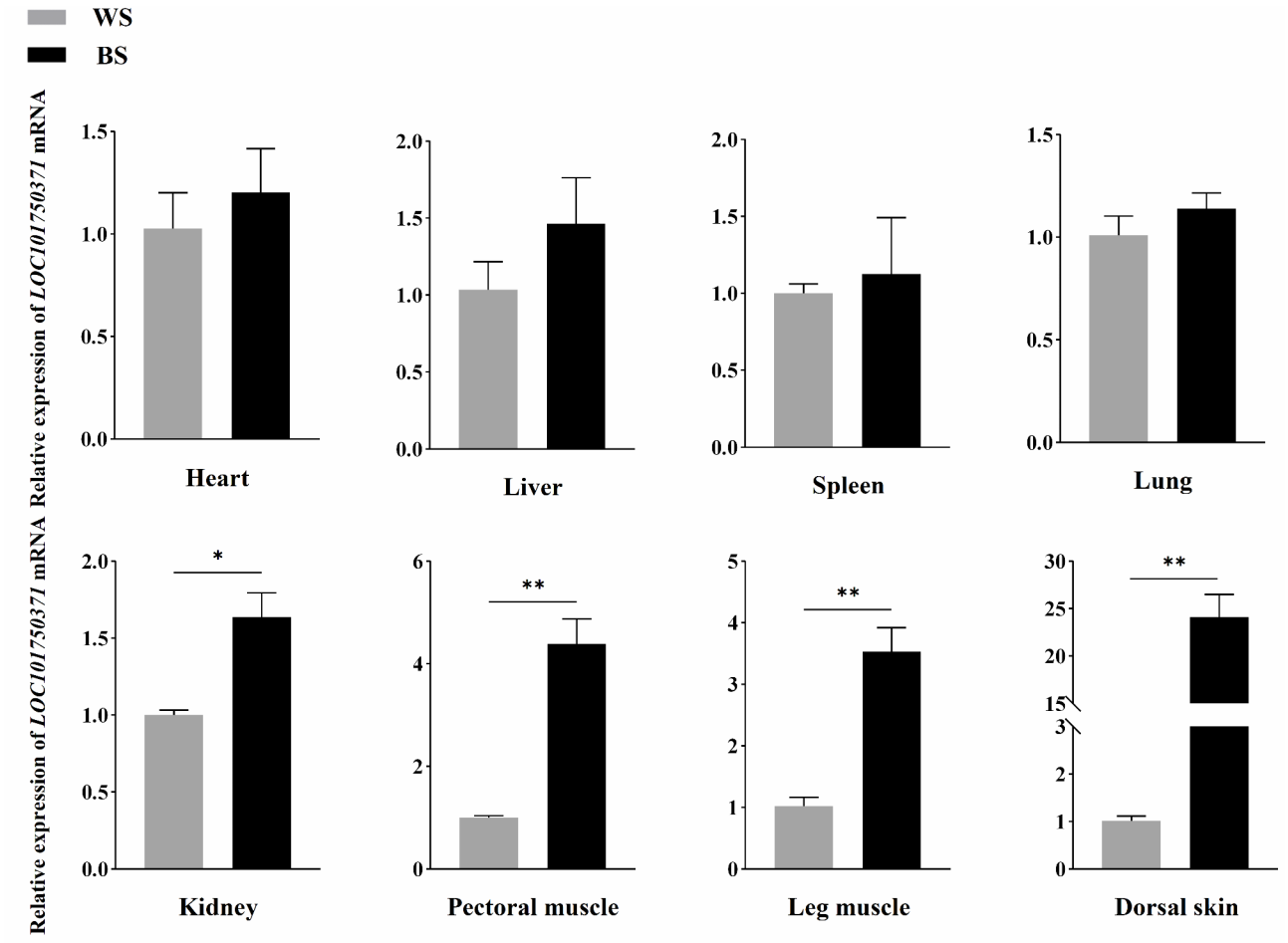

Fig. 8 Comparative expression of *LOC101750371* gene in different tissues of Luning chickens with white skin and black skin. WS represents the white skin, and BS represents the black skin. *$P < 0.05$, **$P < 0.01$

indicating that SNPs significantly associated with skin color were mainly concentrated in chr20 and chrZ. A number of genes that have been reported to play important regulatory functions in melanin synthesis and deposition were identified on these regions: *ATP5E*, *EDN3*, *ELMO2*, *GNAS*, *TUBB1*, *MTAP*, *CDKN2A*, *CDKN2B*, *TRIM36*, *NRG1*, *CTSV*, and *FER*. Additionally, the previously unreported *LOC101750371* and *LOC121108313* were identified in the 68.24–68.58 Mb interval where chrZ is most strongly selected. These genes, along with genes enriched for GO terms associated with pigmentation such as *GNAQ*, *KITLG*, *MCHR1*, and *TYR*, were considered candidate genes for WGRS screens (Fig. 4b).

Transcriptome sequencing has a wide range of applications in exploring poultry characterization mechanisms, disease research, and nutrition [37–39]. To better investigate the mechanism of pigmentation, we performed RNA-seq of a phenotypically mutated white skin Luning chicken along with three other black skin Luning chickens. We identified 2045 DE mRNAs, 2763 DE lncRNAs, and 110 DE pre-miRNAs between WS group and BS group. By predicting the target genes of lncRNAs, it is possible to gain insights into how lncRNAs affect cellular functions by regulating the expression of these genes, which helps to reveal the roles and mechanisms of action of lncRNAs in the regulatory network of gene expression [40]. miRNAs affect post-transcriptional regulation of mRNAs mainly through interactions with the target genes, causing degradation or transcriptional repression of the mRNAs [41]. This study was to further screen the key genes affecting skin pigmentation by predicting the target genes of DE lncRNAs and DE pre-miRNAs. Then, we predicted the target genes of DE lncRNAs and DE pre-miRNAs, and the target genes and DE mRNAs were analyzed by GO enrichment analysis, and identified 12 genes enriched in pigmentation associated GO terms. These includes genes that have been verified to be involved in regulating coat color and skin color: agouti signaling protein (*ASIP*), *TYR*, tyrosinase related protein 1 (*TYRP1*), premelanosome protein (*PMEL*), melan-A (*MLANA*), solute carrier family 45 member 2 (*SLC45A2*), and KIT proto-oncogene, receptor tyrosine kinase (*KIT*) [42–44].

This study combines WGRS and RNA-seq to uncover the genetic factors associated with the coloring process in chickens and screen for candidate genes affecting skin color traits in black-bone chickens. 50 DE mRNAs, 37 DE lncRNAs target genes, and 199 DE pre-miRNAs target genes were found to overlap with WGRS strongly selected genes. Additionally, 29 genes were present in all four data sets (Fig. 5d). Three of these genes, *ATP5E*, *EDN3*, and *LOC101750371*, were also part of the previously identified WGRS candidates. Li et al. [9] integration of whole-genome and transcriptome data identified *SLC45A2*, *SLMO2*, *ATP5E* and *EDN3* as candidate genes for melanin deposition. Endothelin (EDN) is a family of active peptides produced by endothelial cells, including three endothelin peptides: EDN1, EDN2 and EDN3. *EDN3* plays a role in promoting the proliferation and differentiation of early neural crest cell precursors that generate melanocytes [45]. Previous studies have suggested that *EDN3* is a candidate gene for pigmentation in various animals such as chickens [34], ducks [46], and mice [47]. Additionally, the uncharacterized *LOC101750371* in candidate genes is not only a differentially expressed RNA in RNA-seq but also highly selected in WGRS. However, further investigation is needed to determine its regulatory role in pigmentation.

This study initially explored the structure of the protein, but the function of the gene requires further experimental verification. By detecting the expression of *LOC101750371* in different tissues of black-skin Luning chickens, it was found that its expression in the dorsal skin was significantly higher than that in the other 7 tissues, followed by the pectoral and leg muscles. This result is consistent with the fact that Luning chicken is an black-bone chicken with black beak, skin and meat, and provides theoretical basis for the role of *LOC101750371* in melanin deposition. We also found that the expression of *LOC101750371* in the pectoral muscle, leg muscle and dorsal skin tissues of black-skin Luning chickens was highly significantly higher than that of white-skin Luning chicken. This result also further demonstrated the existence of a regulatory effect of *LOC101750371* on the mechanism of melanin deposition in Luning chickens.

Conclusion

In summary, we performed WGRS on five individual Luning chickens to evaluate genomic diversity, evolutionary history, and signal selection in various local breeds. Our findings indicated that the 68.24–68.58 Mb genomic region on chrZ was significantly associated with pigmentation traits in black-bone chicken. Through integrated genomic and transcriptomic analysis, we identified *ATP5E*, *EDN3* and *LOC101750371* as potential influencers of pigmentation in chickens. And preliminary evidence for the existence of a regulatory effect of *LOC101750371* on the mechanism of melanin deposition in Luning chickens. This study has the potential to accelerate the breeding process of Luning chickens, and the identified candidate genes can contribute to understanding the molecular mechanism of pigmentation.

Methods

Sample collection and resequencing

In this experiment, all the Luning chicken samples in this experiment were provided by Sichuan Luning chicken genetic resources breeding farm. Whole blood samples

were collected from five 94-day-old male black-bone chickens in Luning chickens. Approximately 2.0 ml of blood was collected from the inferior wing vein and stored in a cryovial with EDTA, then promptly placed in a liquid nitrogen tank. Genomic DNA was isolated using TIANamp Genomic DNA Kit. Non-contaminated DNA samples (Supplementary Table S9 & Supplementary Fig. S7) were used for library construction using the TruSeq DNA LT Sample Prep kit. The DNA fragments underwent end repaired, A-tailed, ligated, purification, PCR amplification, and other steps to finalize the library construction. Sequencing was performed using the DNBSEQ-T7 sequencer to generate raw data. During the experiment, it was observed that one male Luning chicken (150-day-old) exhibited a phenotypic mutation to white color. Three black-bone Luning chickens of the same age were selected to assess the dorsal skin luminance values (L) of the four individuals. Heart, liver, spleen, lung, kidney, pectoral muscle, leg muscle and dorsal skin tissues were collected for RNA extraction, and dorsal skin tissue for RNA-seq; cDNA synthesis using PrimeScript™ RT reagent Kit with gDNA Eraser (Perfect Real Time). All four individuals were euthanized and samples were collected in a sterile environment. The pentobarbital was used for euthanization by intraperitoneal injection at dose of 40 mg/kg of chicken body weight [48].

Including the data from current research, we also obtained sequence data from the NCBI database for 35 individuals from other chicken breeds (Supplementary Table S10) [8, 9, 21, 49, 50]. Thus, there were 40 chickens in total (5 individuals per breed), including Luning chickens (LNC), Tibetan chickens (TBC), Pengxian yellow chickens (PYC), Jiuyuan black-bone chickens (JBC), and Muchuan black-bone chickens (MBC) all from Sichuan, Xichuan black-bone chickens (XBC) from Henan, Silkie chickens (SC) from Jiangsu, and Red junglefowl (RJF) from Yunnan.

Quality control processing and variant calling

Quality filtering of sequencing reads was performed using the default parameters of fastp [51] software, quality filtering standards: remove adaptors, trim reads with bases≥5 (non AGCT), trim nucleotides having an average base correct recognize rate less than 99% within a window of 4 nucleotides. Lastly, reads with lengths less than 75 bp or average quality score less than 15 were removed. Clean reads were aligned to the reference genome (https://ftp.ncbi.nlm.nih.gov/genomes/all/GCF/016/699/485/GCF_016699485.2_bGalGal1.mat.broiler.GRCg7b/GCF_016699485.2_bGalGal1.mat.broiler.GRCg7b_genomic.fna.gz) using BWA [52], after converting the comparison result format using SAMtools [53], Picard (https://broadinstitute.github.io/picard/) was used to remove redundancy, and the results were compared and analyzed using Qualimap [54]. Single nucleotide polymorphisms (SNPs) and insertion/deletion sequences (InDels) were identified using GATK [55]. Gene annotation of SNPs and InDels deletion results was performed using Annovar [56]. The parameters of GATK for SNPs were set as follows: QD<2.0 || MQ<40.0 || FS>60.0 || SOR>3.0 || MQRankSum < -12.5 || ReadPosRankSum < -8.0, and the parameters for InDels were set as follows: QD<2.0 || MQ<40.0 || FS>200.0 || SOR>10.0 || ReadPosRankSum < -20.0. The detected SNPs and InDels of LNCs are integrated into Circos map for visual presentation of genomic data. Cluster analysis has proceeded via the R package (ComplexHeatmap) [57].

Population structure

First, genome-wide SNPs were filtered by PLINK (set the parameters to: --indep-pairwise 50 5 0.5) and non-closely linked SNPs were selected for population structure analysis [58]. The IBS matrix was calculated using PLINK based on filtered genome-wide SNPs sites, and then a phylogenetic tree was constructed for all samples using neighbor-joining (NJ) in PHYLIP [59]. We made the principal component analysis (PCA) via the software EIGENSOFT [60]. The Admixture analysis was performed using ADMIXTURE [61] program according to K=2 to K=5. 10 different seeds were selected for 10 replicate analyses, and then pong [62] was used to cluster the 10 results, and representative results were selected for plotting. ADMIXTURE suggests determining the optimal K based on Cross-Validation error.

Runs of homozygosity and linkage disequilibrium analysis

The runs of homozygosity (ROH) were identified by the runs of the homozygosity tool in detectRUNS [63] to count individual-level and group-level ROH in the window-free case. Dividing the seven breeds of chickens into black-bone chickens (LNC, XBC, MBC, SC) and non-black-bone chickens (TBC, PYC, RJF) for linkage disequilibrium (LD) analysis. We conducted the correlation coefficient r^2 with the software PopLDdecay [64].

Demographic history

To detect changes in the effective ancestral population sizes of the LNC, we first extracted all the typing sites for 28 individuals (samples sequenced to a depth greater than 20× and with relatively pure ancestral components) of seven populations from the BAM file and used the SNPable pipline (https://lh3lh3.users.sourceforge.net/snpable.shtml) to create a total breeds mask file. Moreover, we used shapeit4 [65] to dichotomize all samples, integrating all phased and unphased sites in the samples, and used the Multiple Sequentially Markovian

Coalescent 2 (MSMC2) tool [66] to do a population dynamic history analysis with a generation time (g) of 1 year and a mutation rate (μ) of 1.91×10^{-9} per generation [67].

Selective sweep analysis

To ascertain the candidate regions for melanin deposition after targeted selection in the LNC, the *Fst* and $\theta\pi$ ratios between black-bone chickens (LNC, XBC, MBC, SC) and non-black-bone chickens (TBC, PYC, RJF) were calculated by VCFtools [57]. We calculated the average *Fst* value and $\theta\pi$ ratios in 200 kb sliding windows with a 20 kb sliding step. The top 5% of the *Fst* value and $\theta\pi$ ratios were selected as the selected region. Finally, Gene Ontology (GO) functional annotation of the candidate genes in the selected region, followed by the corresponding enrichment analysis.

RNA-seq and data analysis

To better screen for melanin-related genes, dorsal skin from 4 chickens were constructed in specific libraries and performed RNA-seq. RNA-seq was performed using the Illumina sequencing platform and raw data were stored in fastq format. The data were compared to the chicken reference genome (GRCg7b) using HISAT2 software (http://ccb.jhu.edu/software/hisat2/index.shtml) [68] after quality control by fastp. The software StringTie (http://ccb.jhu.edu/software/stringtie/) [69] was used to assemble and splice the mapped reads and functionally annotate of potential new transcripts.

White skin Luning chicken (WS) was used as the control group and black skin Luning chickens (BS) were used as the treatment group, and the expression levels of the genes and transcripts were quantitatively analyzed using RSEM software, respectively. Then we calculated TPM (Transcripts Per Million reads) according to the gene length and read numbers. Differentially expressed mRNAs (DE mRNAs), differentially expressed lncRNAs (DE lncRNAs), and differentially expressed pre-miRNAs (DE pre-miRNAs) were detected with DEGseq using a threshold of $P_{adj} < 0.001$ and $|\log_2 FC| \geq 2$. DE lncRNAs target gene prediction was performed, and neighboring protein-coding genes within 10 kb upstream and downstream of DE lncRNAs were identified as cis-acting target genes. On the other hand, DE lncRNAs and DE mRNAs correlation coefficients (r) were calculated, and DE lncRNAs with $|r|>0.8$ and $P_{adj} < 0.05$ were identified as trans-acting target genes. Prediction of target genes for DE pre-miRNAs using the software miRanda [70] (https://github.com/hacktrackgnulinux/miranda), the parameters were set as follows: -sc 160 -en -20 -strict.

Validation of DE RNAs by qRT-PCR

To ensure the accuracy of RNA-seq, quantitative real-time polymerase chain reaction (qRT-PCR) analysis was used to determine the expression level of randomly selected mRNAs, lncRNAs, and pre-miRNAs (5 each). Total RNA was reverse transcribed according to the reverse transcription kit (PrimeScript™ RT reagent Kit with gDNA Eraser) to obtain cDNA. The qRT-PCR primers were designed by Primer Premier 5 and are shown in Supplementary Table S11. The qRT-PCR 20-μL reaction consisted of 10 μL 2×Taq Pro Universal SYBR qPCR Master Mix, 0.4 μL of each primer, 2 μL of cDNA, 7.2 μL of ddH_2O. The amplification conditions consisted of 95 ℃ for 30 s, followed by 30 cycles of 95 ℃ for 10 s, and 60 ℃ for 30 s. A melting curve procedure consisted of 95 ℃ for 15 s, 60 ℃ for 1 min, and 95 ℃ for 15 s. Three technical replicates were set for each sample, and the relative expression was calculated by the $2^{-\Delta\Delta Ct}$ method using *GAPDH* (used for mRNA and lncRNA) and *U6* (used for pre-miRNAs) as the internal reference gene. The results obtained are expressed using mean±standard error. $P<0.05$ were defined as significant and $P<0.01$ were highly significant.

Cloning and analysis of the Luning chicken *LOC101750371* gene

The dorsal skin tissues of the black-skin Luning chicken were used as a template to clone the *LOC101750371* gene, and the amino acid sequence was predicted using DNAMAN software. SOPMA was used to predict the secondary structure of LOC101750371 protein, SWISS-MODEL was used to predict the tertiary structure, ExPASy ProtScale was used to predict the hydrophilicity of the protein, SignalP-4.1 was used to predict the protein phosphorylation site, NetNGlyc-1.0 was used to predict the protein N-glycosylation site, the YinOYang-1.2 was used to predict protein O-glycosylation sites.

Using *GAPDH* as an internal reference gene, qRT-PCR was used to detect the relative expression of *LOC101750371* gene in heart, liver, spleen, lung, kidney, pectoral muscle, leg muscle and dorsal skin tissues of black-skin Luning chickens, and to compare the relative expression of *LOC101750371* gene in different tissues of white-skin and black-skin Luning chickens. The qRT-PCR reaction system and reaction conditions were consistent with those of "Validation of DE RNAs by qRT-PCR". Three technical replicates were set for each sample, and the relative expression was calculated by the $2^{-\Delta\Delta Ct}$ method. The primers for quantitative detection are shown in Supplementary Table S11.

Abbreviations

WGRS	Whole-genome resequencing
RNA-seq	Transcriptome sequencing
LNC	Luning chicken

TBC	Tibetan chicken
PYC	Pengxian yellow chicken
XBC	Xichuan black-bone chicken
JBC	Jiuyuan black-bone chicken
MBC	Muchuan black-bone chicken
SC	Silkie chicken
RJF	Red junglefowl
SNPs	Single nucleotide polymorphisms
InDels	Insertion/deletion sequences
NJ	Neighbor-joining
PCA	Principal component analysis
ROH	Runs of homozygosity
LD	Linkage disequilibrium
L	Luminance
BS	Black skin
WS	White skin
DE mRNAs	Differentially expressed mRNAs
DE lncRNAs	Differentially expressed lncRNAs
DE pre-miRNAs	Differentially expressed pre-miRNAs
GO	Gene Ontology

Supplementary Information

The online version contains supplementary material available at https://doi.org/10.1186/s12864-024-10774-5.

Supplementary Material 1

Supplementary Material 2

Supplementary Material 3

Supplementary Material 4

Supplementary Material 5

Supplementary Material 6

Supplementary Material 7

Supplementary Material 8

Supplementary Material 9

Supplementary Material 10

Supplementary Material 11

Supplementary Material 12

Supplementary Material 13

Acknowledgements
Not applicable.

Author contributions
CWC and ZXL conceived and designed the research. CWC performed the experiments. JL, ZYL, YN, JYW, and ZW collected the samples and analyzed the data. CWC wrote the manuscript. All the authors have read and approved the final manuscript.

Funding
This work was supported by the Science and Technology Support Program of Sichuan Province (2021YFYZ0031 and 2023YFSY0048), the Natural Science Foundation of Sichuan Province (2023NSFSC1142), and the Fundamental Research Funds for the Central Universities of Southwest Minzu University (ZYN2023095).

Data availability
The raw data for the 5 Luning chickens used in the whole-genome resequencing, and for the 4 Luning chickens used in the transcriptome are accessible at NCBI under BioProject accession numbers PRJNA954999 and PRJNA1059763, respectively. The other 35 chickens used in this study were downloaded from NCBI with BioProject accession numbers PRJNA642410, PRJNA241474, PRJNA800119, PRJNA597842, and PRJNA306389.

Declarations

Ethics approval and consent to participate
All animal studies were approved by the Institutional Animal Care and Use Committee of Southwest Minzu University (Certification No. 2022MDLS44). The authors declare that all animal experiments were carried out in compliance with the ARRIVE guidelines for the reporting of animal experiments. The study involved only farm owned chickens, and informed consent was obtained from the chicken farm for their participation in this study.

Consent for publication
Not applicable.

Competing interests
The authors declare no competing interests.

Received: 9 January 2024 / Accepted: 4 September 2024
Published online: 13 September 2024

References

1. Purugganan P M. What is domestication? Trends Ecol Evol. 2022;37(8):663–71. https://doi.org/10.1016/j.tree.2022.04.006.
2. Leif A, Michael P. Molecular genetic variation of animals and plants under domestication. Proc Natl Acad Sci USA. 2022;119(30). https://doi.org/10.1073/pnas.2122150119.
3. Fang MY, Larson G, Ribeiro HS, Li N, Andersson L. Contrasting mode of evolution at a coat color locus in wild and domestic pigs. PLoS Genet. 2009;5(1):e1000341. https://doi.org/10.1371/journal.pgen.1000341.
4. Wang MS, Zhang RW, Su LY, Li Y, Peng MS, Liu HQ, et al. Positive selection rather than relaxation of functional constraint drives the evolution of vision during chicken domestication. Cell Res. 2016;26(5):556–73. https://doi.org/10.1038/cr.2016.44.
5. Duan S, Niu L, Yin T, Li L, Gao S, Yuan D, et al. A novel strategy for screening bioavailable quality markers of traditional Chinese medicine by integrating intestinal absorption and network pharmacology: application to Wu Ji Bai Feng Pill. Phytomedicine. 2020;76:153226. https://doi.org/10.1016/j.phymed.2020.153226.
6. Liao XJ, Shi XW, Hu HM, Han XJ, Jiang K, Liu Y, et al. Comparative metabolomics analysis reveals the unique nutritional characteristics of breed and feed on muscles in Chinese Taihe black-bone silky fowl. Metabolites. 2022;12(10):914. https://doi.org/10.3390/metabo12100914.
7. Zhang ZR, Li GM, Wei Y, Feng ZY, Fang L, Li ML, et al. In vitro immunomodulatory and antioxidant effects of oligopeptides and four characteristic peptides in black-bone silky fowl (Gallus gallus Domesticus Brisson). J Food Biochem. 2022;46(12):e14469. https://doi.org/10.1111/jfbc.14469.
8. Shi S, Shao D, Yang L, Liang Q, Han W, Xue Q, et al. Whole genome analyses reveal novel genes associated with chicken adaptation to tropical and frigid environments. J Adv Res. 2022;47:13–25. https://doi.org/10.1016/j.jare.2022.07.005.
9. Li D, Sun G, Zhang M, Cao Y, Zhang C, Fu Y, et al. Breeding history and candidate genes responsible for black skin of Xichuan black-bone chicken. BMC Genomics. 2020;21(1):511. https://doi.org/10.1186/s12864-020-06900-8.
10. Cai Z, Sarup P, Ostersen T, Nielsen B, Fredholm M, Karlskov-Mortensen P, et al. Genomic diversity revealed by whole-genome sequencing in three Danish commercial pig breeds. J Anim Sci. 2020;98(7):skaa229. https://doi.org/10.1093/jas/skaa229.
11. Ros-Freixedes R, Johnsson M, Whalen A, Chen CY, Valente BD, Herring WO, et al. Genomic prediction with whole-genome sequence data in intensely selected pig lines. Genet Selection Evol. 2022;54(1):65. https://doi.org/10.1186/s12711-022-00756-0.
12. Zhang S, Yao Z, Li X, Zhang Z, Liu X, Yang P, et al. Assessing genomic diversity and signatures of selection in Pinan cattle using whole-genome sequencing data. BMC Genomics. 2022;23(1):460. https://doi.org/10.1186/s12864-022-08645-y.
13. Lv FH, Cao YH, Liu GJ, Luo LY, Lu R, Liu MJ, et al. Whole-genome resequencing of worldwide wild and domestic sheep elucidates genetic diversity, introgression, and agronomically important loci. Mol Biol Evol. 2022;39(2):msab353. https://doi.org/10.1093/molbev/msab353.

14. Liu Z, Tan X, Wang J, Jin Q, Meng X, Cai Z, et al. Whole genome sequencing of Luxi Black Head sheep for screening selection signatures associated with important traits. Anim Bioscience. 2022;35(9):1340–50. https://doi.org/10.5713/ab.21.0533.
15. Gu L, Wang F, Lin Z, Xu T, Lin D, Xing M, et al. Genetic characteristics of Jiaji duck by whole genome re-sequencing. PLoS ONE. 2020;15(2):e0228964. https://doi.org/10.1371/journal.pone.0228964.
16. Wang W, Wang F, Hao R, Wang A, Sharshov K, Druzyaka A, et al. First de novo whole genome sequencing and assembly of the bar-headed goose. PeerJ. 2020;8:e8914. https://doi.org/10.7717/peerj.8914.
17. Makanjuola BO, Maltecca C, Miglior F, Marras G, Abdalla EA, Schenkel FS, et al. Identification of unique ROH regions with unfavorable effects on production and fertility traits in Canadian holsteins. Genet Selection Evol. 2021;53(1):68. https://doi.org/10.1186/s12711-021-00660-z.
18. Kim S-J, Lü JM, Yi S, Choi T, Kim B-M, Lee BY, et al. Climate response over Asia/Arctic to change in orbital parameters for the last interglacial maximum. Geoscience J. 2010;14(2):173–90. https://doi.org/10.1007/s12303-010-0017-1.
19. Koparde P, Mehta P, Mukherjee S, Robin VV. Quaternary climatic fluctuations and resulting climatically suitable areas for eurasian owlets. Ecol Evol. 2019;9(8):4864–74. https://doi.org/10.1002/ece3.5086.
20. Lan D, Xiong X, Mipam TD, Fu C, Li Q, Ai Y et al. Genetic diversity, Molecular Phylogeny, and selection evidence of Jinchuan Yak revealed by whole-genome resequencing. G3 (Bethesda). 2018;8(3):945–52. https://doi.org/10.1534/g3.118.300572
21. Li D, Che T, Chen B, Tian S, Zhou X, Zhang G, et al. Genomic data for 78 chickens from 14 populations. Gigascience. 2017;6(6):1–5. https://doi.org/10.1093/gigascience/gix026.
22. Eda M, Lu P, Kikuchi H, Li Z, Li F, Yuan J. Reevaluation of early Holocene chicken domestication in northern China. J Archaeol Sci. 2016;67:25–31. https://doi.org/10.1016/j.jas.2016.01.012.
23. Miao YW, Peng MS, Wu GS, Ouyang YN, Yang ZY, Yu N, et al. Chicken domestication: an updated perspective based on mitochondrial genomes. Heredity (Edinb). 2013;110(3):277–82. https://doi.org/10.1038/hdy.2012.83.
24. Sun J, Chen T, Zhu M, Wang R, Huang Y, Wei Q, et al. Whole-genome sequencing revealed genetic diversity and selection of Guangxi indigenous chickens. PLoS ONE. 2022;17(3):e0250392. https://doi.org/10.1371/journal.pone.0250392.
25. Hung CM, Shaner PJ, Zink RM, Liu WC, Chu TC, Huang WS, et al. Drastic population fluctuations explain the rapid extinction of the passenger pigeon. Proc Natl Acad Sci USA. 2014;111(29):10636–41. https://doi.org/10.1073/pnas.1401526111.
26. Guo Q, Jiang Y, Wang Z, Bi Y, Chen G, Bai H, et al. Genome-wide analysis identifies candidate genes encoding beak color of duck. Genes (Basel). 2022;13(7):1271. https://doi.org/10.3390/genes13071271.
27. Tian D, Han B, Pei Q, Zhou B, Wang L, Li X, et al. Whole genome sequencing identified candidate genes related to litter size of Qinghai fine wool sheep under artificial selection. Small Ruminant Res. 2023;223:106969. https://doi.org/10.1016/j.smallrumres.2023.106969.
28. Ouyang J, Wu Y, Li Y, Miao J, Zheng S, Tang H, et al. Identification of key candidate genes for wing length-related traits by whole-genome resequencing in 772 geese. Br Poult Sci. 2022;63(6):747–53. https://doi.org/10.1080/00071668.2022.2102889.
29. Xiong G, Chen W, Jiang K, Liu S, Li J, Liao X. Integrated transcriptome and proteome analysis reveals the unique molecular features and nutritional components on the muscles in Chinese Taihe black-bone silky fowl chicken. PLoS ONE. 2024;19(3):e0299385. https://doi.org/10.1371/journal.pone.0299385.
30. Khumpeerawat P, Duangjinda M, Phasuk Y. Factors affecting gene expression associated with the skin color of black-bone chicken in Thailand. Poult Sci. 2021;100(11):101440. https://doi.org/10.1016/j.psj.2021.101440.
31. Zhang XD, Wang HH, Zhang CX, Li QH, Chen XH, Lou LF. Analysis of skin color change and related gene expression after crossing of Dongxiang black chicken and ISA layer. Genet Mol Res. 2015;14(3):11551–61. https://doi.org/10.4238/2015.September.28.7.
32. Li G, Li D, Yang N, Qu L, Hou Z, Zheng J, et al. A genome-wide association study identifies novel single nucleotide polymorphisms associated with dermal shank pigmentation in chickens. Poult Sci. 2014;93(12):2983–7. https://doi.org/10.3382/ps.2014-04164.
33. Hou H, Wang X, Zhang C, Tu Y, Lv W, Cai X, et al. Genomic analysis of GBS data reveals genes associated with facial pigmentation in Xinyang blue-shelled layers. Archives Anim Breed. 2020;63(2):483–91. https://doi.org/10.5194/aab-63-483-2020.
34. Cha J, Jin D, Kim JH, Kim SC, Lim JA, Chai HH, et al. Genome-wide association study revealed the genomic regions associated with skin pigmentation in an ogye x White Leghorn F2 chicken population. Poult Sci. 2023;102(8):102720. https://doi.org/10.1016/j.psj.2023.102720.
35. Perini F, Cendron F, Lasagna E, Cassandro M, Penasa M. Genomic insights into shank and eggshell color in Italian local chickens. Poult Sci. 2024;103(6):103677. https://doi.org/10.1016/j.psj.2024.103677.
36. Li J, Bed'hom B, Marthey S, Valade M, Dureux A, Moroldo M, et al. A missense mutation in TYRP1 causes the chocolate plumage color in chicken and alters melanosome structure. Pigment Cell Melanoma Res. 2019;32(3):381–90. https://doi.org/10.1111/pcmr.12753.
37. Dan-dan W, Yan-yan Z, Meng-lin T, Zhang W, Chun-lin X, Ke-ren J, et al. Integrative analysis of hypothalamic transcriptome and genetic association study reveals key genes involved in the regulation of egg production in indigenous chickens. J Integr Agric. 2022;21(05):1457–74. https://doi.org/10.1016/S2095-3119(21)63842-X.
38. Zamzam SH, Ghalyanchilangeroudi A, Khosravi AR. Comparative trachea transcriptome analysis in SPF broiler chickens infected with avian infectious bronchitis and avian influenza viruses. Virus Genes. 2022;58(3):203–13. https://doi.org/10.1007/s11262-022-01893-w.
39. Cao X, Wang Y, Shu D, Qu H, Luo C, Hu X. Food intake-related genes in chicken determined through combinatorial genome-wide association study and transcriptome analysis. Anim Genet. 2020;51(5):741–51. https://doi.org/10.1111/age.12980.
40. Chiu HS, Somvanshi S, Chen TW, Sumazin P. Illuminating lncRNA function through target prediction. Methods Mol Biol. 2021;2372:263–95. https://doi.org/10.1007/978-1-0716-1697-0_22.
41. Bartel DP. MicroRNAs: target recognition and regulatory functions. Cell. 2009;136(2):215–33. https://doi.org/10.1016/j.cell.2009.01.002.
42. Rajawat D, Panigrahi M, Nayak SS, Ghildiyal K, Sharma A, Kumar H et al. Uncovering genes underlying coat color variation in indigenous cattle breeds through genome-wide positive selection. Animal Biotechnol. 2023:1–14. https://doi.org/10.1080/10495398.2023.2240387
43. Xu M, Tang S, Liu X, Deng Y, He C, Guo S, et al. Genes influencing deposition of melanin in breast muscle of the Xuefeng black bone chicken based on bioinformatic analysis. Genome. 2023;66(8):212–23. https://doi.org/10.1139/gen-2022-0090.
44. Li R, Wang Y, Liu Y, Li D, Tian Y, Liu X, et al. Effects of SLC45A2 and GPNMB on melanin deposition based on transcriptome sequencing in chicken feather follicles. Anim (Basel). 2023;13(16):2608. https://doi.org/10.3390/ani13162608.
45. Lahav R, Ziller C, Dupin E, Le Douarin NM. Endothelin 3 promotes neural crest cell proliferation and mediates a vast increase in melanocyte number in culture. Proc Natl Acad Sci USA. 1996;93(9):3892–7. https://doi.org/10.1073/pnas.93.9.3892.
46. Lin R, Li J, Zhao F, Zhou M, Wang J, Xiao T. Transcriptome analysis of genes potentially associated with white and black plumage formation in Chinese indigenous ducks (Anas platyrhynchos). Br Poult Sci. 2022;63(4):466–74. https://doi.org/10.1080/00071668.2022.2035676.
47. Li H, Fan L, Zhu S, Shin MK, Lu F, Qu J, et al. Epilation induces hair and skin pigmentation through an EDN3/EDNRB-dependent regenerative response of melanocyte stem cells. Sci Rep. 2017;7(1):7272. https://doi.org/10.1038/s41598-017-07683-x.
48. Yang M, Hu B, Sun D, Zhao C, Wei H, Li D, et al. Growth hormone receptor gene influences mitochondrial function and chicken lipid metabolism by AMPK-PGC1α-PPAR signaling pathway. BMC Genomics. 2022;23(1):219. https://doi.org/10.1186/s12864-021-08268-9.
49. Wang MS, Li Y, Peng MS, Zhong L, Wang ZJ, Li QY, et al. Genomic analyses reveal potential independent adaptation to high altitude in tibetan chickens. Mol Biol Evol. 2015;32(7):1880–9. https://doi.org/10.1093/molbev/msv071.
50. Guo Y, Ou JH, Zan Y, Wang Y, Li H, Zhu C, et al. Researching on the fine structure and admixture of the worldwide chicken population reveal connections between populations and important events in breeding history. Evol Appl. 2022;15(4):553–64. https://doi.org/10.1111/eva.13241.
51. Chen S, Zhou Y, Chen Y, Gu J. Fastp: an ultra-fast all-in-one FASTQ preprocessor. Bioinformatics. 2018;34(17):i884–90. https://doi.org/10.1093/bioinformatics/bty560.
52. Bolger AM, Lohse M, Usadel B. Trimmomatic: a flexible trimmer for Illumina sequence data. Bioinformatics. 2014;30(15):2114–20. https://doi.org/10.1093/bioinformatics/btu170.
53. Li H, Handsaker B, Wysoker A, Fennell T, Ruan J, Homer N, et al. The sequence alignment/map format and SAMtools. Bioinformatics. 2009;25(16):2078–9. https://doi.org/10.1093/bioinformatics/btp352.

54. Okonechnikov K, Conesa A, García-Alcalde F. Qualimap 2: advanced multi-sample quality control for high-throughput sequencing data. Bioinformatics. 2016;32(2):292–4. https://doi.org/10.1093/bioinformatics/btv566.
55. McKenna A, Hanna M, Banks E, Sivachenko A, Cibulskis K, Kernytsky A, et al. The genome analysis toolkit: MapReduce framework for analyzing next-generation DNA sequencing data. Genome Res. 2010;20(9):1297–303. https://doi.org/10.1101/gr.107524.110.
56. Wang K, Li M, Hakonarson H. ANNOVAR: functional annotation of genetic variants from high-throughput sequencing data. Nucleic Acids Res. 2010;38(16):e164. https://doi.org/10.1093/nar/gkq603.
57. Gu ZG, Eils R, Schlesner M. Complex heatmaps reveal patterns and correlations in multidimensional genomic data. Bioinf (Oxford England). 2016;32(18):2847–9. https://doi.org/10.1093/bioinformatics/btw313.
58. Purcell S, Neale B, Todd-Brown K, Thomas L, Ferreira MA, Bender D, et al. PLINK: a tool set for whole-genome association and population-based linkage analyses. Am J Hum Genet. 2007;81(3):559–75. https://doi.org/10.1086/519795.
59. Plotree D, Plotgram D. PHYLIP-Phylogeny inference package (version 3.2). Cladistics. 1989;5:163–6.
60. Price AL, Patterson NJ, Plenge RM, Weinblatt ME, Shadick NA, Reich D. Principal components analysis corrects for stratification in genome-wide association studies. Nat Genet. 2006;38(8):904–9. https://doi.org/10.1038/ng1847.
61. Alexander DH, Novembre J, Lange K. Fast model-based estimation of ancestry in unrelated individuals. Genome Res. 2009;19(9):1655–64. https://doi.org/10.1101/gr.094052.109.
62. Behr AA, Liu KZ, Liu-Fang G, Nakka P, Ramachandran S. Pong: fast analysis and visualization of latent clusters in population genetic data. Bioinformatics. 2016;32(18):2817–23. https://doi.org/10.1093/bioinformatics/btw327.
63. Marras G, Gaspa G, Sorbolini S, Dimauro C, Ajmone-Marsan P, Valentini A, et al. Analysis of runs of homozygosity and their relationship with inbreeding in five cattle breeds farmed in Italy. Anim Genet. 2015;46(2):110–21. https://doi.org/10.1111/age.12259.
64. Zhang C, Dong SS, Xu JY, He WM, Yang TL. PopLDdecay: a fast and effective tool for linkage disequilibrium decay analysis based on variant call format files. Bioinformatics. 2019;35(10):1786–8. https://doi.org/10.1093/bioinformatics/bty875.
65. Delaneau O, Zagury JF, Robinson MR, Marchini JL, Dermitzakis ET. Accurate, scalable and integrative haplotype estimation. Nat Commun. 2019;10(1):5436. https://doi.org/10.1038/s41467-019-13225-y.
66. Schiffels S, Wang K, MSMC, MSMC2. The multiple sequentially markovian coalescent. Methods in Molecular Biology. (Clifton NJ). 2020;2090:147–66. https://doi.org/10.1007/978-1-0716-0199-0_7.
67. Nam K, Mugal C, Nabholz B, Schielzeth H, Wolf JB, Backström N, et al. Molecular evolution of genes in avian genomes. Genome Biol. 2010;11(6):R68. https://doi.org/10.1186/gb-2010-11-6-r68.
68. Grabherr MG, Haas BJ, Yassour M, Levin JZ, Thompson DA, Amit I, et al. Nat Biotechnol. 2011;29(7):644–52. https://doi.org/10.1038/nbt.1883. Full-length transcriptome assembly from RNA-Seq data without a reference genome.
69. Li W, Godzik A. Cd-hit: a fast program for clustering and comparing large sets of protein or nucleotide sequences. Bioinformatics. 2006;22(13):1658–9. https://doi.org/10.1093/bioinformatics/btl158.
70. Enright AJ, John B, Gaul U, Tuschl T, Sander C, Marks DS. MicroRNA targets in Drosophila. Genome Biol. 2003;5(1):R1. https://doi.org/10.1186/gb-2003-5-1-r1.

Publisher's note